

Electrostatic Background of Chromatin Fiber Stretching

<http://www.jbsdonline.com>

Nikolay Korolev^{1**}
Alexander P. Lyubartsev^{2*}
Aatto Laaksonen²

¹School of Biological Sciences
Nanyang Technological University
60 Nanyang Drive
637551 Singapore
²Division of Physical Chemistry
Arrhenius Laboratory
Stockholm University
S 106 91
Stockholm, Sweden

Abstract

We have carried out an investigation of the electrostatic forces involved in gradual removal of the DNA from the histone proteins in chromatin. Two simple models of DNA – histone core dissociation were considered. Calculations of the electrostatic free energy within the Poisson-Boltzmann theory gave similar results for the both models, which turned out to be in a qualitative agreement with recent optical tweezers stretching experiments measuring the force necessary to unwrap DNA from the histone core. Our analysis shows that the electrostatic interactions between the highly negatively charged polymeric DNA and the positively charged histones play a determining role in stabilizing the nucleosomes at physiological conditions.

Key words: Nucleosome, Single-molecule experiment, Histone-DNA interactions, Polyelectrolytes

Introduction

In eukaryotic cells, DNA, the carrier of genetic information is confined in the nucleus and exists in the form of DNA-protein complexes known as chromatin. About 85% of DNA in the chromatin is represented by uniform units, the nucleosomes, complexes of 160-230 base pairs (bp) of DNA double helix with five proteins, called histones and abbreviated as H2A, H2B, H3, H4, and H1 (1). The most regular central part of the nucleosome is called the nucleosome core particle (NCP) and consists of 147 bp DNA wrapped as a 1.75 turn super-helix around a wedge-like hetero-octamer of the four highly conserved core histones. The histone octamer is formed from the two H2A/H2B dimers and one (H3/H4)₂ tetramer (2, 3). Variable length (10-80 bp) linker DNA connects the NCPs to each other and binds to the linker histone H1 (or its variants). The linear arrays of the nucleosomes are further compacted on higher levels of chromatin organization (still poorly understood). The histones are responsible for the first step of DNA compaction in chromatin and pose a major obstacle for direct access to the DNA of proteins responsible for DNA replication, transcription, repair, and recombination. Clearly understanding the mechanisms behind assembly and disassembly of the nucleosomes is of great importance for life science.

Recent optical tweezers stretching experiments (4, 5) of a single DNA molecule, assembled into a linear array of the nucleosomes, have beautifully revealed the molecular mechanisms and the ranges of the mechanical forces involved in a DNA unwrapping from the histones. The results of these measurements will certainly inspire to further investigation to uncover the “mechanical action” of various molecular motors working on DNA, *e.g.*, helicases, RNA polymerases or virus

*Email: sasha@phyc.su.se

**Email: korolev@ntu.edu.sg

packaging proteins. Two distinct regions were observed on the force-extension curves by Brower-Toland *et al.* (4): a low-force region (with forces $F < 15$ pN), where the unwinding of the DNA double helix proceeds gradually from the nucleosome core and a second region of higher forces $F \sim 25 - 30$ pN, where the last 80 bp of DNA (roughly, one turn of the DNA superhelix) are spontaneously released from the histones in an all-or-nothing manner. To explain the appearance of the latter high-force transition, an especially strong binding of the DNA to the histone octamer was assumed at the symmetrical position between ± 3.5 and ± 4.5 DNA helical turns from the dyad axis (the DNA in the NCP is mapped on DNA helical turns from -7 to +7 assigning 0 for a position at the dyad axis of the superhelix (3, 6)). This binding mode is expected to create an energetic barrier for a smooth gradual DNA unwinding (4, 7). This mechanism is in line with a general view of the properties of the NCP as an interplay between the behavior of DNA as a rigid, unevenly bent (and “bendable”) polymer, and the existence of 12-14 strong binding sites on the lateral surface of the histone octamer (6, 8-10).

In the process of unwrapping DNA from histones two charged polyelectrolyte entities are formed: densely negatively charged DNA and positively charged histone core. It is clear that electrostatic interactions arising in such a case must have a profound influence on the course of whole process and on equilibrium between the two phases. The electrostatic forces resist the detachment of the DNA from the histones during the single-chromatin fiber stretching under the influence of a mechanical pulling force. The degree of this resistance is dependent not only on the strength of the individual histone core – DNA contacts but also on the ionic conditions in the solution as well as on the balance between the positively and negatively charged groups in the chromatin. Other important contributions to the detachment process, the mechanical bending force and specific short-range DNA-histone interactions, are much less dependent on the ionic conditions.

Despite the fact that the electrostatic interactions must have a determining influence on DNA unwrapping, their role is rarely discussed in the literature. The aim of our paper is to analyze the electrostatic component of the DNA-histone interactions within the NCP. We calculate the contribution of the electrostatic forces to a formation of the elementary structural unit of chromatin, the nucleosome, using the mean theory (Poisson Boltzmann) approximation and discuss the obtained results in relation to the recent DNA stretching experiments.

Results and Discussion

Thermodynamic Aspects

The nucleosome core particle represents a non-stoichiometric polyanion-polycation complex where the total negative charge on the DNA (147 bp with 294 charged phosphate groups) is approximately *twice* the net positive charge of the histone core (+146 formed by 218 Lys⁺ and Arg⁺ with 72 Glu⁻ and Asp⁻). Therefore, substantial electrostatic forces are involved in the dissociation/association processes of either the entire NCP or its subgroups (the histone N-terminal tails, H2A/H2B dimers and (H3/H4)₂ tetramer). The unwinding of DNA from the histones can be presented through multiple dissociation reactions of oligocation-polyanion complexes according to:



Here L^{Z+} is the basic domain of the DNA-binding protein with a total positive charge $Z+$, while M^+ and A^- are cations and anions, respectively, of the 1-1 salt, like KCl or NaCl. B and B_L are the numbers of M^+ and A^- ions, thermodynamically bound to the dissociated DNA^{N-} polyanion and the ligand L^{Z+} , respectively. Thermodynamic binding includes all modes of interactions, *i.e.*, site-specific non-

ionic binding, creation of inner-sphere complexes (direct cation-anion pairs), solvent-separated cation-anion interactions, as well as diffuse electrostatic localization of fully hydrated cations in the vicinity of the polyanion due to its electric field.

In Figure 1, the degree of dissociation from a double stranded (ds) DNA is shown for the positively charged amino acid fragments as a function of salt concentration. We have used the data from the measurements of the oligolysine/oligoarginine binding (11) to the dsDNA to calculate the amount of free ligands, based on the well-established (both in experiments and theoretical studies) linear dependence of the logarithm of the binding constant K_{obs} per ligand L^{Z+} on $\log C_M$

$$\log K_{obs} = \log K(1M) - bZ \cdot \log C_M \quad [2]$$

Here $K(1M)$ is the K_{obs} value, extrapolated to $C_M = 1M$ while bZ is the slope of the $\log K_{obs} - \log C_M$ line with b being the thermodynamic degree of the M^+ ion association with the polyion per unit charge. For a double-helical DNA b is given a constant value about 0.9 in a wide range of salt concentration (11, 12). The salt dependence of K_{obs} , described by Eq. [2], has been shown to be valid for the majority of specific and non-specific DNA-binding proteins (13).

Figure 1 implies that at the thermodynamic equilibrium under the salt condition of the chromatin fiber stretching experiments, neither the octamer (+146), nor the $(H3/H4)_2$ (+76) tetramer, the H2A/H2B (+35) dimers, nor even histone tails (with the net charge ranging from +9 to +13) become completely detached from the DNA. Therefore some efforts are needed to dissociate polycation-polyanion complexes of such a large total charge. It can be done by, *e.g.*, increasing the salt concentration to shield the DNA charge from the histones, raising temperature, through work done by ATP consuming proteins (helicases, polymerases), or by mechanical force in single-molecule stretching experiments. Below we will use simple theoretical models to estimate difference in electrostatic free energy between the intact nucleosome and its components (DNA and histone octamer) free in solution. This difference gives evaluation of the minimum work against electrostatic forces, which should be performed by any of the above listed means. At the same time, a population of dissociated oligocations (histone subdomains with $Z = +2 - +4$) does exist at physiological salt concentrations. These dissociated cationic groups are responsible for *internal* dynamic behavior of the NCP. While the nucleosome itself can be considered as a stable polycation-polyanion complex, its positively charged subgroups can easily exchange their electrostatic “partners” through a partial dissociation/association of their sub-domains. This conclusion can be drawn from an analysis of existing experimental data without invoking any theoretical assumptions, where we have used the data by Lohman and co-workers (11, 14), obtained with the fluorescent quenching method. This technique most probably underestimates the thermodynamic degree of the ligand binding since it detects only the population of the most tightly bound oligopeptides.

Nucleosome Unwinding:

Non-stoichiometric Binding Model

The experimental data on L^{Z+} binding to the polynucleotides are usually interpreted by applying common polyelectrolyte theories (13), assuming 1:1 charge balance to the DNA-basic protein complex. A more general *non-stoichiometric* oligocation-polyanion binding has been much less analyzed so far. Consider now a change in the free energy of the electrostatic interaction of the polyion with the mobile ions in solution upon formation of its non-stoichiometric complex with the ligand L^{Z+} . This change, calculated per one charged group of the *ligand* is:

$$\Delta g_{L}^{el} = (g_{C}^{el} - g_{F}^{el}) \cdot (N/Z) \quad [3]$$

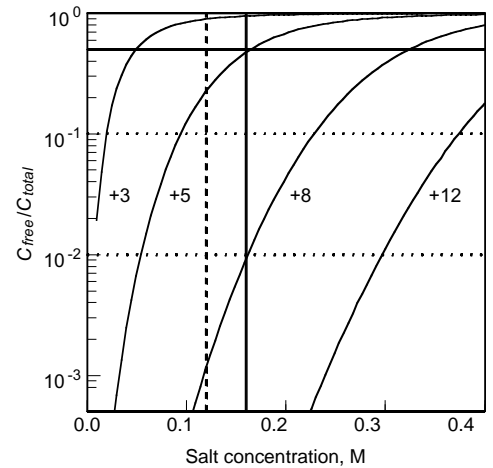


Figure 1: Estimation of the population of the dissociated protein domains (C_{free}/C_{total}) for several domain charges (marked in the figure) with a varied salt concentration. The solid and dashed vertical bars correspond to the salt conditions applied in the stretching experiments, reported by Brower-Toland *et al.* (4) and by Bennink *et al.* (5), respectively. Two dotted and one solid horizontal bars show 1%, 10%, and 50% ligand dissociation, respectively. The DNA concentration (C_p) is 1 mM phosphates, the oligocation ligand concentration (C_{total}) is chosen to neutralize 50% of the DNA charge ($C_{total} = C_p/2Z$), the values of K_{obs} are calculated from the data reported by Mascotti and Lohman (11).

Here g_C^{el} and g_F^{el} are the free energies of the polyion – mobile ion interactions (calculated per unit charge of the *polyion*), respectively, in the $[L^{Z+} \cdot DNA^{N-}]$ complex and in the “free state” of DNA before the ligand binding; N is the number of charged groups of the polyion forming the binding site of the L^{Z+} ligand. Assuming the uncharged state of the ligand-polyion complex as a reference level for calculation of the electrostatic free energy; for the case when the charge of the ligand completely neutralizes the charge of the binding site on the polyion ($N=Z$) we have $g_C^{el} = 0$, and $\Delta g_L^{el} = -g_F^{el}$. When the ligand L^{Z+} forms a complex with the polyion by occupying a part of the polyion with a charge larger than its own (when $N > Z$), then the polyion-ligand complex retains the negative charge $Z - N$ and interacts with ionic surrounding resulting in $g_C^{el} \neq 0$ in Eq. [3].

To evaluate Δg^{el} numerically we introduce some further approximations. First, the discretely charged polyions are replaced by uniformly charged cylinders of the same dimension both for the free DNA and the ligand-DNA complex. DNA in the NCP is considered as a cylinder with the charge partially compensated by the ligands (histones). Secondly, we neglect interaction of the ligand L^{Z+} with simple salt, which was justified in previous experimental and theoretical works on non-specific oligocation-DNA binding with charges of the ligands typical for the histone domains such as flexible histone tails with charge around +10 (see (15) and references cited therein).

Some support for application of this primitive model to such a complex object as nucleosome can be given from detailed consideration of the distribution of the positive charges in histones. The most of the histone charge (+88 of total +146) is located in the flexible unstructured N-terminal domains (called the histone tails), which protrude from the DNA wrapped on the histone octamer and therefore are able to interact with the DNA similar to the simple charged ligands like polyamines (16). The rest of the positive charge of the histone is within the folded domains inside the NCP. However, the most of them are placed on the surface of the octamer directing DNA wrapping (2). Being very close to the DNA, these Lys⁺/Arg⁺ residues “switch off” the charge of the DNA phosphate groups facing the histones. Other forces, such as the DNA bending, mutual repulsion of the DNA polyions on the lateral surface of the octamer, as well as contributions from formation of ion pairs, specific histone-DNA contacts and influence of solvent (water) molecules are not included in this very primitive model.

When the DNA is unwrapping from the histone core, the number of DNA charge groups N in the NCP is decreasing while the charge of ligands Z remains constant. We compute the electrostatic free energy by combining two terms: DNA still remaining in the NCP (with charge $Z-N$ and length Nl , $l=1.7$ Å being the axial distance between the DNA charged groups) and free DNA (charge $N-N_c$ and length $(N_c-N)l$, $N_c \approx 300$ being the number of DNA charges in the completely bound NCP). We assume that the ligand charge is evenly distributed over the polyion binding site. The free energy of each term is computed as for an infinitely long cylinder (per unit length) and then is multiplied by the length of the corresponding fragment. The values of g_C^{el} and g_F^{el} include both the enthalpy and entropy terms and can be calculated using PB cell model as described in the corresponding section below.

Nucleosome Unwinding: Primitive Model

Yet another simplified model can be used to estimate the electrostatic contribution to the process of unwinding the DNA polyion from the positively charged histone core. The nucleosome core particle can be approximated as a charged sphere. An intact nucleosome has a net negative charge of about -150. A detachment of the DNA from the NCP increases the NCP charge and simultaneously exposes the stretched DNA polyion to the solvent. In the course of unwinding, the charge of the (roughly) spherical NCP increases from -150, passing the point of the charges of DNA and histone

are equal so that the total charge of the NCP cancels out to zero. Complete stretching of the chromatin fiber results in a dissociation of the NCP and ends with the histone octamer completely detached from DNA, corresponding to a positively charged sphere of net charge about +150 and a free DNA of roughly 150 bp length carrying a charge of -300. This allows us to calculate the electrostatic energy of the nucleosome at different degrees of unwinding ($r \in [0,1]$) as a sum of electrostatic energy of the sphere with charge $Q(r) = -150 + r \cdot 300$ and the DNA polyion of the variable length and charge $N(r) = -300 \cdot r$, neglecting the contribution from the regions of close proximity of the detached DNA and the NCP and ignoring alteration of the NCP size and the dissociation of the octamer after the release of the DNA. To calculate the numerical values of the DNA and NCP electrostatic free energy we use the same Poisson Boltzmann polyelectrolyte model as in the approach described above. The above model is similar to some other simple models suggested earlier (17-19) which use analytical approaches or simple polyelectrolyte theories to predict binding of the excessive charge of DNA on the histone core modeled as charged sphere.

Poisson-Boltzmann Cell Model and Electrostatic Free Energy

To estimate the contribution of the electrostatics to the formation of the complex between the DNA and the positively charged ligands we need to compare the electrostatic free energy (ΔG^{el}) of the interaction of the DNA polyion with the monovalent ions in the solution before and after the formation of the complex with the positively charged ligand, L^{Z+} .

Assuming volume change $\Delta V^{el} = 0$; $\Delta G^{el} = \Delta E^{el} - T \cdot \Delta S^{el}$, where the electrostatic energy change, $\Delta E^{el} = E_f^{el} - E_c^{el}$ and $\Delta S^{el} = S_f^{el} - S_c^{el}$ is the change in the electrostatic entropy. The indices f and c are for the respective DNA states as a “free” polyion (without attached ligand L^{Z+}) and in a ligand-DNA complex. The Poisson-Boltzmann (PB) cell model (20-23) is used for calculation of the terms contributing to ΔG^{el} . According to this model, the solvent is treated as a continuum with a constant dielectric permittivity, which depends only on temperature. DNA is approximated as an infinitely long and uniformly charged cylinder of radius a with a unit charge spacing l ; the NCP is modeled as sphere with a radius c and the total charge Q . The small monovalent ions are treated as impenetrable hard spheres. In the PB approach, the radii of the counterions and coions determine only the closest distance to the polyion, and do not produce any excluded volume effects near the surface of the polyion.

The electrostatic internal energy per charged group of the polyelectrolyte, associated with introducing a polyion into the system, is calculated by (see, e.g., (24)):

$$E^{el}/kT = -\frac{1}{2} |\psi(a)| + \frac{1}{2} \int_V d^3\vec{r} \sum_{\alpha} (Z_{\alpha} \rho_{\alpha}(\vec{r})) \psi(\vec{r}) \quad [4]$$

The electrostatic entropy contribution due to redistribution of the ions around the charged polyion is given by:

$$S^{el}/k = -l_0 \int_V d^3\vec{r} \sum_{\alpha} \left[\rho_{\alpha}(\vec{r}) \ln \left(\frac{\rho_{\alpha}(\vec{r})}{C_{\alpha}^0} \right) \right] \quad [5]$$

In Eqs. [4] and [5], $\psi(r) = e\phi(\vec{r})/kT$ is the reduced electrostatic potential, a is the radius of the polyion; integration is carried out over the cell (cylindrical or spherical) of radius R (except the space occupied by the polyion) and defined by the polyion concentration. In the Poisson-Boltzmann approximation, the ion density distribution of α -species of ions $\rho_{\alpha}(\vec{r}) = C_{\alpha}^0 \exp(-Z_{\alpha} \psi(\vec{r}))$, with C_{α}^0 being the concentration of α ions at the outer cell boundary where the potential $\psi(\vec{r})$ is assumed to be zero. $l_0 = e^2/(\epsilon kT)$ is the so-called Bjerrum length. The values of C_{α}^0 and the electrostatic potential $\psi(\vec{r})$ as a function of coordinate can be in a stan-

dard manner calculated for the given parameters of the polyion and concentration of species. The resulting functions of electrostatic potential $\psi(\vec{r})$ and ion density distribution $\rho_\alpha(\vec{r})$ allow the determination of the electrostatic energy and entropy components of the free energy by Eqs. [4] and [5] (25). Note, that in the systems of spherical or cylindrical symmetry, integration in formulas [4] and [5], as well as in numerical solution of the PB equation, can be reduced to one-dimensional integration over the radial coordinate. Other details of the computational procedure can be found in our earlier work (16, 25, 26).

For the double stranded DNA, we use structural parameters we have already successfully applied in our earlier works: $l = 1.7 \text{ \AA}$, $a = 9.5 \text{ \AA}$ (25, 27). The ion radius was 2 \AA which is close to those determined for Na^+ and Cl^- (28), for Mg^{2+} , 3 \AA is used as an ion radius (29). For the DNA-ligand complex, we used the same radius as for free DNA while the charge density was defined by the charge of the bound ligand. The NCP is a complex of the wedge-like histone octamer with the DNA wrapped on its lateral surface as a 1.75 turn superhelix. It looks like a short cylinder of 55 \AA with a 110 \AA diameter. We model the NCP particle as a sphere of radius 50 \AA which gives a volume and a surface area close to the values of a real NCP. The concentration of the salts was taken from the work on chromatin fiber stretching: 155 mM NaCl (5) or $110 \text{ mM NaCl} + 1.5 \text{ mM MgCl}_2$ (4).

Despite many inherent approximations, free energy calculations using this rather simple PB polyelectrolyte theory have been successfully used by many authors to describe experimental data on polyelectrolyte structural transitions accompanied by changes of the charge density of the polyion. In particular, free energy calculations within the PB cell model give an adequate description of the influence of Mg^{2+} on structural equilibria between single-, double-, and triple-stranded DNA and RNA polynucleotides in dependence on temperature and the Na^+ or K^+ concentration (25, 27). Using this approach we were able to trace the differences in binding of Mg^{2+} , K^+ , and Na^+ to DNA and RNA which was also confirmed by experimental data (26). Recently, a similar PB model in combination with assumptions about a non-stoichiometric ligand binding has been applied to explain the counter-intuitive dependence of the thermal helix-coil transition of DNA in the presence of the triple-charged polyamines upon variation of the polyamines length (16).

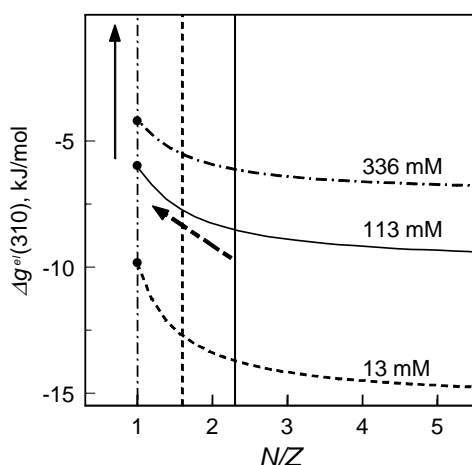


Figure 2: Estimation of the electrostatic $\text{LZ}^+\text{-DNA}^{\text{N-}}$ complex formation free energy, calculated per unit charge of the ligand at 310 K with respect to the charge stoichiometry of the oligocation-polyanion complex N/Z ratio. The solid and dashed vertical bars show the estimations of the N/Z ratio in the nucleosomal arrays reported by Brower-Toland *et al.* (4) and by Bennink *et al.* (5), respectively. See the text for details.

Non-stoichiometric Charge Balance and Stability of Ligand-polyelectrolyte Complexes

First we estimate the ligand-DNA electrostatic free energy by taking into account the non-stoichiometric charge balance in the $[\text{LZ}^+\text{-DNA}]$ complex. In agreement with the result of earlier work (30, 31), the calculations based on Eqs. [4], [5] show that a stoichiometric binding of the ligand to the polyion ($Z=N$) is not the most thermodynamically favorable situation. To illustrate this, the change in the free energy of the polycation-polyanion complex at three different salt concentrations is shown in Figure 2 as a function of the N/Z ratio.

Formation of the stoichiometric ($N/Z=1$) from the completely dissociated state leads to electrostatic energy gain about -6 kJ/mol for each positive charge of the ligand LZ^+ at physiological salt concentration (Fig. 2). That gives roughly $\Delta G^{\text{el}} \approx -900 \text{ kJ/mol}$ per nucleosome. With the increase of the N/Z ratio the absolute value of $\Delta g^{\text{el}}_{\text{L}}$ additionally amplifies. The electrostatic free energy of complex formation becomes approximately 1.6-1.7 times more favorable at $N/Z \rightarrow \infty$ compared with $N/Z = 1$. The most of the additional gain in the free energy is achieved when $N/Z \leq 3$. A further increase of the ligand size makes its binding to DNA only slightly more favorable. Effect of “non-stoichiometric stabilization” contributes by an additional $\Delta G^{\text{el}} \approx -340 \text{ kJ/mol}$ gain in free energy (assuming $N/Z \approx 2$ in the NCP). This way the electrostatic free energy of the nucleosome formation is very large and favorable,

$\Delta G^{el} \approx -1240$ kJ/mol. This value is very large compared to some experimental data but in agreement with the estimation of the second primitive model (see below).

The result obtained using this fairly approximate approach is supported by the work by other authors (30) who have shown that the application of a similar PB theory with a non-stoichiometric ligand-polyion binding reproduces *quantitatively* the experimental data obtained in the studies of oligolysines binding to a polyion for MCl concentration up to 1 M. Notably, the change in N/Z does not alter the linear dependence of $\log K_{obs}$ on $\log C_M$. It is worth mentioning also that the design of natural oligocations, the histone tails, corresponds to the most effective DNA binding stoichiometry: Lys⁺ and Arg⁺ residues are distributed quite uniformly along the histone tails with an averaged charge density close to the optimal $N/Z \approx 3$ (30).

The origin of the observed additional electrostatic stabilization of the complex with an increase of the number of binding sites N is mainly because of an increase of the ligand binding sites on the DNA (even without full switching off the DNA charges) appears to be more favorable than the existence of the ligand-DNA 1:1 complex *plus* a piece of densely charged DNA polyanion (with $N - Z$ charge). If we analyze the various terms contributing to the free energy difference (Eqs. [4] and [5]) closer, we see that a stabilization of the non-stoichiometric complex while increasing the N/Z ratio is in fact due to a substantial entropic gain from the release of the monovalent cations from the densely charged double helical DNA. This effect can be observed already when the ligand neutralizes a small fraction of the total polyion charge.

Our analysis also shows that the binding of a linear polycation over maximally accessible charges on the surface of the polyanion has a favorable electrostatic component. The higher the charge density on the polyanion surface, the more favorable non-stoichiometric binding becomes, provided that all the other (non-electrostatic) contributions remain the same. Therefore, the tails in the NCP have a tendency to change their positions from the nucleosomal DNA (where $N/Z \approx 2$ that is below an optimal value $N/Z \approx 3$) to the available neighboring polyanions (linker DNA (32), protein acidic domains) where they can achieve a higher N/Z ratio (31).

Estimation of the Change in ΔG^{el} During the Nucleosome Unwinding Within the Primitive Model

Another way to estimate contribution of the electrostatics to the unwinding of the DNA from the histone core is to calculate the change of electrostatic free energy ΔG^{el} , as a sum of free energies of the cylindrical polyion modeling DNA and charged sphere representing NCP. These results are shown in Figure 3.

One can see from Figure 3 that the initial stages of the DNA release from the NCP core are accompanied with small changes in ΔG^{el} because the unfavorable process of exposing the negatively charged DNA to the solvent is accompanied by a simultaneous decrease in ΔG^{el} due to a reduction of the negative charge of the NCP. The relatively small changes in ΔG^{el} during unwinding the first three quarters of the superhelical turn of the DNA increase importance of other forces, such as the DNA bending or “bendability” (8), mutual repulsion of the DNA polyions on the lateral surface of the octamer, as well as other factors, *e.g.*, formation of ion pairs, specific histone-DNA contacts, etc, which are not included in this fairly approximate model. However, the electrostatic forces become dominant when the electroneutrality point of the NCP is reached. After this point, further stripping DNA from the histones becomes thermodynamically strongly unfavorable since it exposes both the negative charges of the DNA polyion and positive charge of the nucleosome core to solvent. (Observe the high values of ΔG^{el} in Fig. 3). The major contribution to ΔG^{el} is the decrease of the entropy due to the confinement of the counterions in the vicinity of the polyelectrolytes. The difference in electrostatic free energy between initial ($Q(0) = -150$; $N(0) = 0$) and final ($Q(I) = +150$; $N(I) = -300$) states of the primitive model

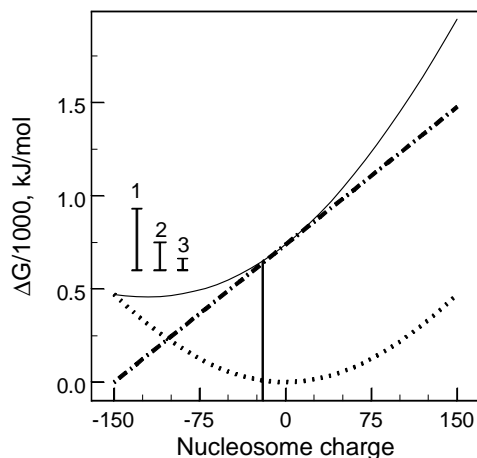


Figure 3: Estimation of changes in electrostatic free energy during nucleosome unwinding in chromatin fiber stretching experiments. Degree of the nucleosome unwinding (abscissa) is measured as change of the total charge of the NCP (histone octamer + DNA attached to it). Dash-dotted line shows the free energy contribution from DNA, released from the octamer during the stretching; dotted line is the electrostatic free energy of the NCP, approximated as a sphere of 50 Å radius (the total charge of the NCP increases from about -150 to +150); solid line is a sum of the two terms. The vertical bar shows the position when one full turn of DNA is wrapped around the histone core. Conditions in solution (salt concentration, temperature) are the same as in the fiber stretching experiment by Brower-Toland *et al.* (4) (similar data, calculated for the salt conditions of work by Bennink *et al.* (5) give very similar curves; not shown). Vertical bars 1-3 are estimations of the energy of DNA bending around the histone core according to (1) ref. 8 (320 kJ/mol); (2) ref. 19 (150 kJ/mol) (3) ref. 33 (62 kJ/mol) and are given to highlight the importance of the electrostatic interactions relative to the DNA bending.

is $\Delta G^{el} \approx -1400 \div -1500$ kJ/mol is in reasonable agreement with the result calculated by the non-stoichiometric ligand-binding model.

Chromatin Fiber Stretching as a Work Against the Electrostatic Force

The Figures 1-3 can be used to illustrate the behavior of the nucleosome during the chromatin fiber stretching experiments by Brower-Toland *et al.* (4). Also, in Figure 4, the qualitative energy profiles illustrate schematically the plausible reaction paths for the process of the nucleosome unwinding under the influence of mechanical pulling force. The “experimental” curves in Figure 4 are in fact not derived from the experiments; they are merely our putative comparison of the energy pass in the single molecule stretching experiments and hypothetical equilibrium process approximated by our simple model. The thin solid line is ΔG^{el} curve, taken from Figure 3 and shows a hypothetical equilibrium. In the beginning of the chromatin fiber stretching, the equilibrium curve is flat, displaying a slow smooth increase when the charge of the NCP approaches zero corresponding to the $N/Z > 1$ region in Figure 2 (indicated by the dashed arrow) or $Q < 0$ in Figure 3. It is then followed by a steeper jump in energy, reflecting the energetic penalty for the creation of an unstable dissociated state of the DNA and histones (vertical arrow in Fig. 2 and steep increase in ΔG^{el} at $Q > 0$ in Fig. 3). In similar fashion we can analyze the reaction paths for the reported stretching experiments. The dashed curve in Figure 4 corresponds to the conditions valid in the work by Bennink *et al.* (5), while the solid thick curve mimics the experiment of Brower-Toland *et al.* (4).

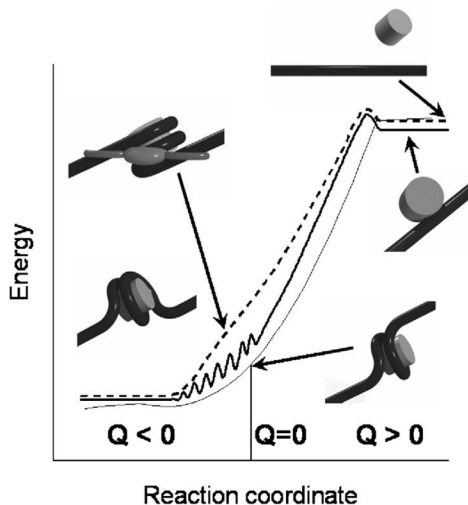


Figure 4: Change of the energy of the NCP in the process of the chromatin fiber unwinding. The thin line displays a hypothetical equilibrium DNA un-wrapping from the nucleosome core; fat solid and dashed curves are estimations of energy passes in single-fiber-pulling experiments from refs. (4) and (5), respectively. The schematic cartoons illustrate the NCP state at different stages of the DNA fiber stretching. The histone tails and dissociation of the histone octamer are not shown. See text for an explanation.

In the beginning of the fiber pulling (at $N/Z \approx 2$), the release of the DNA from the histone core is accompanied by a relatively small energetic penalty since the released positively charged histone groups are able of switching to neutralization of the charge on the remaining DNA. The change in ΔG^{el}_L for this process is shown by dashed arrow in Figure 2. However, the situation changes quite dramatically when the $N/Z=1$ value is reached in a partially unwrapped nucleosome, corresponding roughly to a complete turn of the dsDNA on the histone core. Now, the position in the NCP where the DNA begins to leave an empty lateral surface of the histone octamer (*i.e.*, when less than 1 turn of the DNA is wrapped around the octamer) corresponds not only to the point of electroneutrality of the partially unwound NCP but also matches with the location of the H2A/H2B dimers (7). Clearly, the nucleosome is designed in the way that the electrostatic and structural factors act in a concert during the disassembly and assembly reactions *in vivo*.

In the experiments, carried out by Brower-Toland *et al.* (4), an array of totally 17 nucleosomes was stretched by pulling the fiber at a constant speed of 28 nm/s, whereby two distinct areas in the force-elongation curves could be observed fol-

lowing each other: First, a continuous region at a low force (<15 pN), and thereafter a regular saw-like dependence at $F > 15$ pN, where each peak did correspond to a release of 80 bp of the remaining DNA from the histone octamer. One can therefore assume that during the initial stages of the pulling, the unwinding of the DNA from the NCP proceeds smoothly and is accompanied by a dissociation/association of the histone basic domains without larger perturbations in the amount of the dissociated oligocations. It is also possible that the relocation of the histone tails may take place cooperatively in several steps in such a manner, although any quantitative analysis of this process is not possible under the conditions of the present experiments. Such a release of relatively small DNA stretches has been detected by Bennink *et al.* (5) in the region of low force.

In the last step of the nucleosome unwinding, the energy stored in the deformed DNA pushes most of the histone octamer out of the DNA with a low probability to reassociate due to a high dilution of the system (and due to the flow of solvent). The authors of the original work (4) explain the appearance of all-or-nothing transition in unwinding of the last 80 bp DNA from the histone core by a presence of especially strong binding sites at the symmetrical positions between ± 3.5 and ± 4.5 DNA helical turns from the dyad axis of the NCP. It seems plausible however, taking in mind our analysis of the electrostatic forces, that this specific binding plays a role of a trigger which initiates unwinding of the last 80 bp of DNA, while the force, applied in the stretching experiments performs the work against the electrostatic field.

Comparing the work by Bennink *et al.* (5) to that by Brower-Toland *et al.* (4), there are two main differences which may result in the immediate release of the entire 150 bp DNA from the NCP in one step:

- (i) The pulling in the work by Bennink *et al.* (5) was carried out at very much higher speed (10000 nm/s comparing to 28 nm/s in the work by Brower-Toland *et al.* (4)).
- (ii) The nucleosomal array was obtained using the whole cell extract of *Xenopus laevis* oocytes (Brower-Toland *et al.* (4) have used purified avian core histones).

The extract of *Xenopus laevis* oocytes is known to contain a large amount of other DNA binding proteins, in particular the linker histone B1 (oocyte variant of the histone H1) and the high mobility group protein HMG1 (1). These proteins bind to the nucleosomes at the positions of the DNA exit/entry and therefore are capable to form a kind of a stitch, making the gradual unwinding of DNA quite impossible. Moreover, the presence of the additional DNA-binding proteins in the *Xenopus* oocyte extracts will shift the N/Z proportion in the chromatin fiber closer to the critical value $N/Z = 1$ (e.g., the N- and C-terminal tails of the histone H1 carry a total charge of about +60). The difference in initial state of the nucleosomes constructed in the works (4, 5) is shown in the left-hand inserts of Figure 4 where the top cartoon presents a protein species (like the B1 protein of the *Xenopus* oocyte extract) bound to the NCP and locking the entry/exit of DNA from the histone octamer.

An additional difference in the mechanical behavior of the nucleosomal arrays, observed in the papers (4, 5) is that the stretching of the fiber, generated from the *Xenopus* oocyte extract is to a large degree irreversible, i.e., only a few nucleosomes can be restored after the relief of mechanical stress. In contrast, more nucleosomes were reformed on the relaxed DNA under the conditions applied by Brower-Toland *et al.* (4) although the DNA had lost all the attached histones after several cycles of stretching. We expect that this difference could be due to a higher stored mechanical energy, which was released during a spontaneous extension of the chromatin fiber in the work of Bennink *et al.* (5) with a lower peak in energy in the experiments of Brower-Toland *et al.* (4) (Fig. 4; correspondingly dashed and solid curves). Different states of the fully stretched DNA fiber are shown on the

right hand side of Figure 4 by two cartoons and by different levels of the curves reflecting the cases of full dissociation of the histone (upper line) and each “dash” representing a histone octamer attached to the DNA (the two bottom lines).

Our data on the electrostatic free energy, presented in Figures 2 and 3, allow us to give evaluation of the electrostatic contribution to the total force necessary to remove DNA from NCP. Division of the free energy change may evaluate the force by the length of the released DNA. Within the non-stoichiometric binding model the free change during the first stage of DNA unwinding at conditions of work of Brower-Toland *et al.* (4), corresponds to the dashed arrow in Figure 2 which gives force 22 pN, while the primitive model gives the force 14 pN in the average. The electrostatic free energy change during the second stage of the unwinding (release of the last 80 bp) in the non-stoichiometric binding model corresponds to the value Δg^{el} at $N/Z = 1$ in Figure 2, which at the ionic conditions of work (4) provides the force 50 pN. Evaluation of the force during the second stage of unwinding within the primitive model yields result about 60 pN.

It is worth mentioning that results obtain within the two simple but very different models agree well with each other. The force observed in the DNA stretching experiments is however systematically lower. It is between 5 and 10 pN on the first stage of unwinding (4) and between 20 and 40 pN on the second stage (4, 5). It is clear however that the DNA bending energy favors unwinding and decrease force necessary to remove DNA. According to different evaluations (10, 33), the force due to the bending energy may be between 5 and 20 pN. Subtraction of the bending contribution from the electrostatic force yields the same level of force which was observed in the DNA stretching experiments. Therefore, provided highly approximate models used for estimation of the electrostatic free energy of the nucleosome formation agreement between experimental and theoretical forces can be considered as satisfactory.

The authors of the experimental work (4), from the analysis of dependence of the DNA unwinding force on stretching velocity, estimated the “activation barrier” for the unwinding of the last 80 bp at about 90 kJ/mol (“36–38 $k_B T$ or 21–22 kcal/mol”). By our opinion this estimation appears too low. In particular, the authors perform normalization of the applied mechanical force over all nucleosome particles in the fiber (17 nucleosomes in the beginning of the stretching), considering the force as equally distributed between all NCPs. However, for the linear array of the nucleosomes under stretching *the entire force* is applied to each nucleosome. If the tension were uniformly distributed over the whole fiber then the height of each next peak (critical force for breaking the last 80 bp from octamer) in the saw-like region of the extension-force curve would decrease linearly upon gradual release of each of the 17 nucleosomes and would depend on the initial number of the NCPs in the chromatin fiber. That is not the case as can be seen from the experimental curves of paper by Brower-Toland *et al.* Thus, without “normalization” of the loading force the “activation barrier” becomes about 1500 kJ/mol (for an array of 17 nucleosomes studied in (4)) that is quite in agreement with high electrostatic energy for the nucleosome unwinding estimated in the present work. (Note also, that our analysis specifies that it is not an “activation barrier” but rather a true “climb” to the plateau of much higher energy of the disassembled nucleosome.)

On the first glance, the conclusion about high thermodynamic stability of the nucleosome contradicts also to some experimental observations (34, 35) (and references cited therein) and theoretical models (36, 37) showing spontaneous and complete dissociation of the NCP on free DNA and histones at moderate salt (0.05–0.5 M) and low NCP (0.001–150 nM) concentrations. These data give estimation of absolute stability of NCP at about 45–60 kJ/mol (35). However, an increase in DNA/nucleosome concentration to more physiologically relevant values has lead to the rapid disappearance of NCP dissociation, which was never observed for

chromatin or nucleosomal arrays. Recent paper by Thållström *et al.* (38) refrains the result obtained earlier in this laboratory (35) concluding that histone-DNA binding free energy cannot be measured in dilution-driven dissociation experiments. These experiments may give artificial values for nucleosome stability because of irreversibility of the dissociation process: dissociated DNA has a tendency for spontaneous stretching and becomes effectively separated from the attractive surface of the octamer by high dilution, huge excess of salt, energetic barrier for bending back, etc. Meanwhile, the mentioned above experimental data has provided a basis for general belief that "... in the physiological range of pH, ionic strength and temperature, the core particle is marginally stable" (39). Our estimation of the absolute stability of the NCP is in reasonable agreement with estimations by Manning and co-workers (37, 40) showing that only 6-8% of neutralization of the DNA negative charge by binding to histones is sufficient to compensate for the energetic cost of the DNA bending in the NCP.

Finally we also wish to comment that the conditions of the chromatin-fiber pulling experiments are very much different from those observed during the action of the nucleosome-disassembling machines (RNA polymerases, helicases) *in vivo*. Particularly, very high concentration of the DNA, and the presence of acidic/phosphorylated domains on the histone-contacting surfaces of the chromatin-breaking machines (see recent works reported the structures of helicases (41, 42) or RNA polymerase II (43)) make possible a more smooth transfer and temporary storage of the histones from the DNA taking part in replication or transcription. Mediation of the histone chaperones (nucleoplasmin, nuclear assembly protein 1, N1/N2 proteins) can also facilitate unwinding of the NCP. The results of the electrostatic free energy calculations (see Fig. 3) implicate that supply of the alternative negative charge by the nuclear proteins operating on the nucleosomal template allows to avoid energetically expensive complete dissociation of the NCP by splitting this process on multiply stages. At each stage, the positive charge of the released histones is transferred from DNA to the acidic/phosphorylated domains of the invading protein. More detailed analysis of electrostatic aspects of the transformations in chromatin is presented in our recent work (31).

Acknowledgement

This work is supported by the Swedish Research Council (Vetenskapsrådet).

References and Footnotes

1. A. P. Wolffe, (Ed.) *Chromatin: Structure and Function*, 3rd Edition. Academic Press, San Diego, CA (1998).
2. G. Arents and E. N. Moudrianakis. *Proc. Natl. Acad. Sci. USA* 90, 10489-10493 (1993).
3. K. Luger, A. W. Mader, R. K. Richmond, D. F. Sargent and T. J. Richmond. *Nature* 389, 251-260 (1997).
4. B. D. Brower-Toland, C. L. Smith, R. C. Yeh, J. T. Lis, C. L. Peterson and M. D. Wang. *Proc. Natl. Acad. Sci. USA* 99, 1960-1965 (2002).
5. M. L. Bennink, S. H. Leuba, G. H. Leno, I. Zlatanova, B. G. de Grooth and J. Greve. *Nature Struct. Biol.* 8, 606-610 (2001).
6. K. Luger and T. J. Richmond. *Curr. Opin. Struct. Biol.* 8, 33-40 (1998).
7. J. J. Hayes and J. C. Hansen. *Proc. Natl. Acad. Sci. USA* 99, 1752-1754 (2002).
8. J. Widom. *Q. Rev. Biophys.* 34, 269-324 (2001).
9. U. M. Muthurajan, Y.-J. Park, R. S. Edayathumangalam, S. Chakravarthy, P. N. Dyer and K. Luger. *Biopolymers* 68, 547-556 (2003).
10. K. Luger. *Curr. Opin. Genet. Dev.* 13, 127-135 (2003).
11. D. P. Mascotti and T. M. Lohman. *Biochemistry* 32, 10568-10579 (1993).
12. C. F. Anderson and M. T. Record. *Annu. Rev. Phys. Chem.* 46, 657-700 (1995).
13. M. T. Record, W. Zhang and C. F. Anderson. *Adv. Protein Chem.* 51, 281-353 (1998).
14. T. M. Lohman and D. P. Mascotti. *Methods Enzymol.* 212, 400-424 (1992).
15. W. Zhang, H. Ni, M. W. Capp, C. F. Anderson, T. M. Lohman and M. T. Record. *Biophys. J.* 76, 1008-1017 (1999).
16. N. Korolev, A. P. Lyubartsev and L. Nordenskiöld. *Biophys. Chem.* 104, 55-66 (2003).
17. E. M. Mateescu, C. Jappesen and P. Pincus. *Europhys. Lett.* 46, 493-498 (1999).
18. K.-K. Kunze and R. R. Netz. *Phys. Rev. E* 66, 011918 (2002).

19. H. Schiessel. *J. Phys. Condens. Mat.* 15, R699-R774 (2003).
20. S. Nilsson, L. Piculell and B. Jönsson. *Macromolecules* 22, 2367-2375 (1989).
21. S. Nilsson and L. Piculell. *Macromolecules* 22, 3011-3017 (1989).
22. P. N. Vorontsov-Velyaminov and A. P. Lyubartsev. *J. Biomol. Struct. Dyn.* 7, 739-747 (1989).
23. A. P. Lyubartsev, V. P. Kurmi and P. N. Vorontsov-Velyaminov. *Mol. Biol. (Moscow)* 24, 1532-1538 (1990).
24. D. Stigter. *Biophys. J.* 69, 380-388 (1995).
25. N. Korolev, A. P. Lyubartsev and L. Nordenskiöld. *Biophys. J.* 75, 3041-3056 (1998).
26. N. Korolev, A. P. Lyubartsev and L. Nordenskiöld. *J. Biomol. Struct. Dyn.* 20, 275-290 (2002).
27. J. P. Bond, C. F. Anderson and M. T. Record. *Biophys. J.* 67, 825-836 (1994).
28. W. R. Fawcett and A. C. Tikanen. *J. Phys. Chem.* 100, 4251-4255 (1996).
29. J.-P. Simonin, L. Blum and P. Turq. *J. Phys. Chem.* 100, 7704-7709 (1996).
30. A. V. Sivolob and S. N. Khrapunov. *Mol. Biol. (Moscow)* 22, 414-422 (1988).
31. N. Korolev and L. Nordenskiöld. *Recent Res. Devel. Biophys. Chem.* 2, 103-124 (2001).
32. D. Angelov, J. M. Vitolo, V. Mutskov, S. Dimitrov and J. J. Hayes. *Proc. Natl. Acad. Sci. USA* 98, 6599-6604 (2001).
33. A. Flaus and T. Owen-Hughes. *Biopolymers* 68, 563-578 (2003).
34. T. D. Yager, C. T. McMurray and K. E. van Holde. *Biochemistry* 28, 2271-2281 (1989).
35. J. M. Gottesfeld and K. Luger. *Biochemistry* 40, 10927-10933 (2001).
36. N. L. Marky and G. S. Manning. *Biopolymers* 31, 1543-1557 (1991).
37. N. L. Marky and G. S. Manning. *J. Mol. Biol.* 254, 50-61 (1995).
38. A. Thålsröm, J. M. Gottesfeld, K. Luger and J. Widom. *Biochemistry* 43, 736-741 (2004).
39. K. E. van Holde. *Chromatin*. Springer-Verlag, New York (1989).
40. G. S. Manning. *J. Amer. Chem. Soc.* 125, 15087-15092 (2003).
41. M. R. Sawaya, S. Guo, S. Tabor, C. C. Richardson and T. Ellenberger. *Cell* 99, 167-177 (1999).
42. M. R. Singleton, M. R. Sawaya, T. Ellenberger and D. B. Wigley. *Cell* 101, 589-600 (2000).
43. P. Cramer, D. A. Bushnell and R. D. Kornberg. *Science* 292, 1863-1876 (2001).

Date Received: May 3, 2004

Communicated by the Editor Maxim Frank-Kamenetskii